Supplementary Figure 1

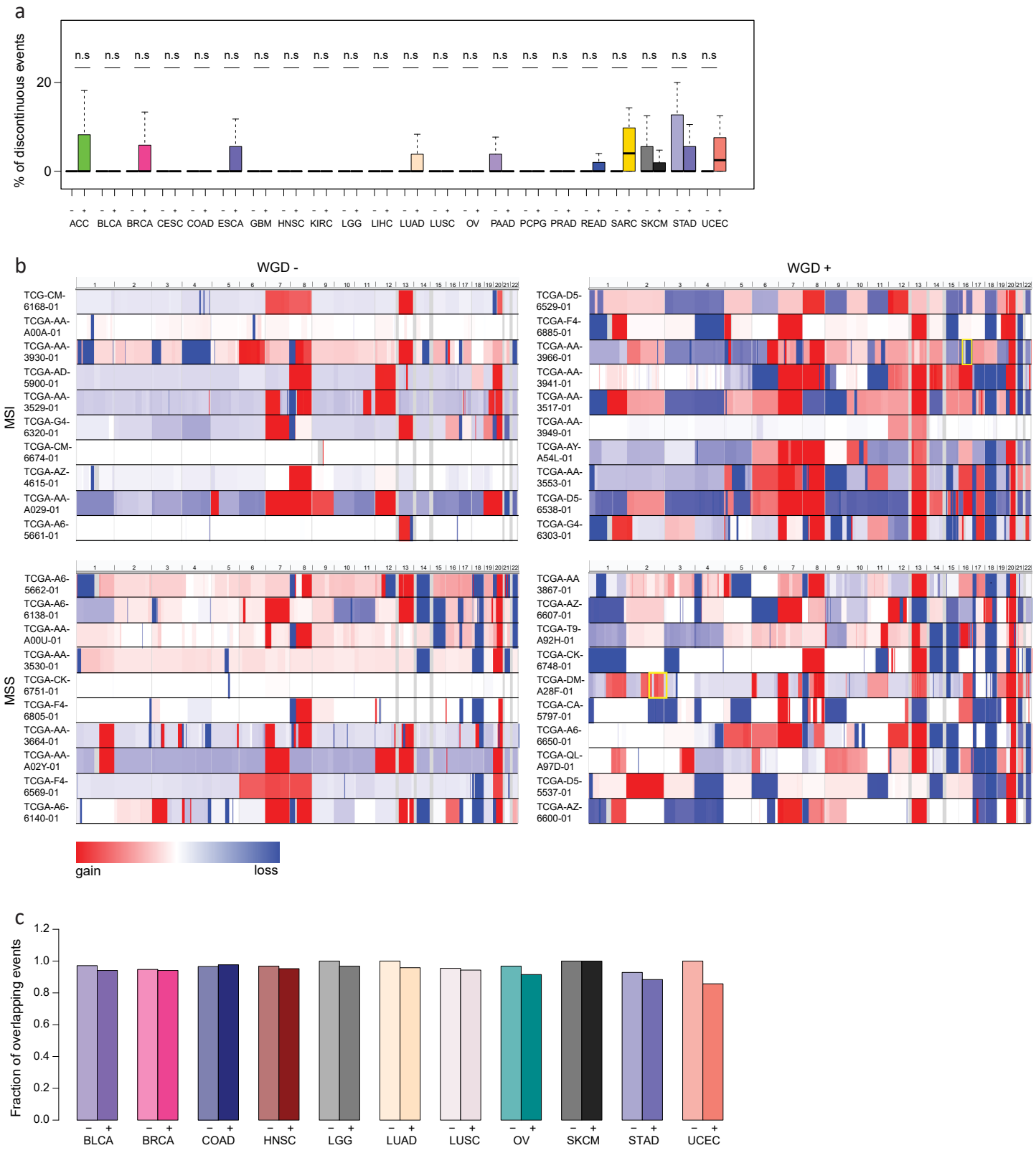

Supplementary Figure 1: Robustness of arm-level aneuploidy calls (related to Figure 1).

(**a**) Comparison of the fraction of chromosome-arm aneuploidies that are discontinuous (have >3 disruptions of the copy number state within the aberration), between WGD- and WGD+ tumors, across the 22 tumor types. 20 samples were randomly selected for each WGD group in each tumor type, and evaluated using IGV visualization. n.s., $p>0.05$. (**b**) IGV-based visualization of 20 MSI/WGD-, 20 MSI/WGD+, 20 MSS/WGD- and 20 MSS/WGD+ COAD samples. MSI, microsatellite instability; MSS, microsatellite stability. The only two discontinuous events that were considered to be chromosome-arm aneuploidies are encircled in yellow. (**c**) The concordance between two GISTIC runs, with the –brlen parameter set to 0.5 or to 0.9, across the 11 tumor types with the highest number of samples. Median overlap = 96.2%.

Supplementary Figure 2

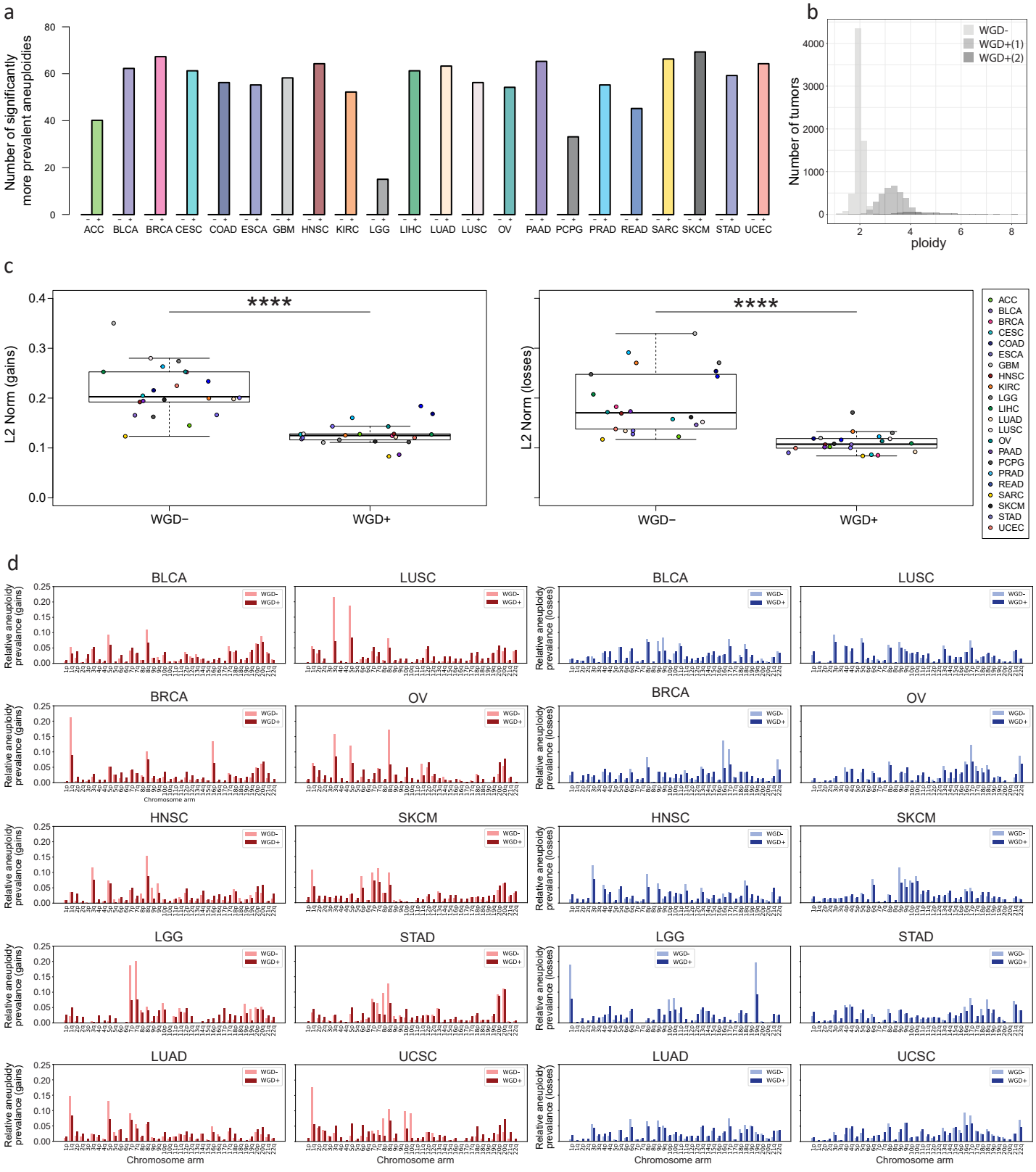

Supplementary Figure 2: The prevalence and general features of aneuploidy in WGD- and WGD+ tumors (related to Figure 1).

(**a**) Comparison of the number of aneuploidies that are significantly ($p<0.05$, $q<0.25$, prevalence $>=0.1$) more prevalent in one WGD group than in the other group. (**b**) Histogram presenting the ploidy distribution of tumors that have not undergone WGD (WGD-), those that have undergone WGD once (WGD+ (1)) and those that have undergone WGD twice (WGD+ (2)). (**c**) Comparison of the deviation of chromosome-arm gains (left) and losses (right) from a uniform distribution, between WGD- and WGD+ tumors, across the 22 tumor types. ****, p=5e-08 and p=2e-07, for gains and losses, respectively; two-tailed paired Student's paired t-test. (**d**) The relative prevalence of chromosome-arm gains (left two columns) and losses (right two columns) in WGD- and WGD+ tumors of 10 selected tumor types. Tumor type abbreviations as in **Fig. 1**.

Supplementary Figure 3

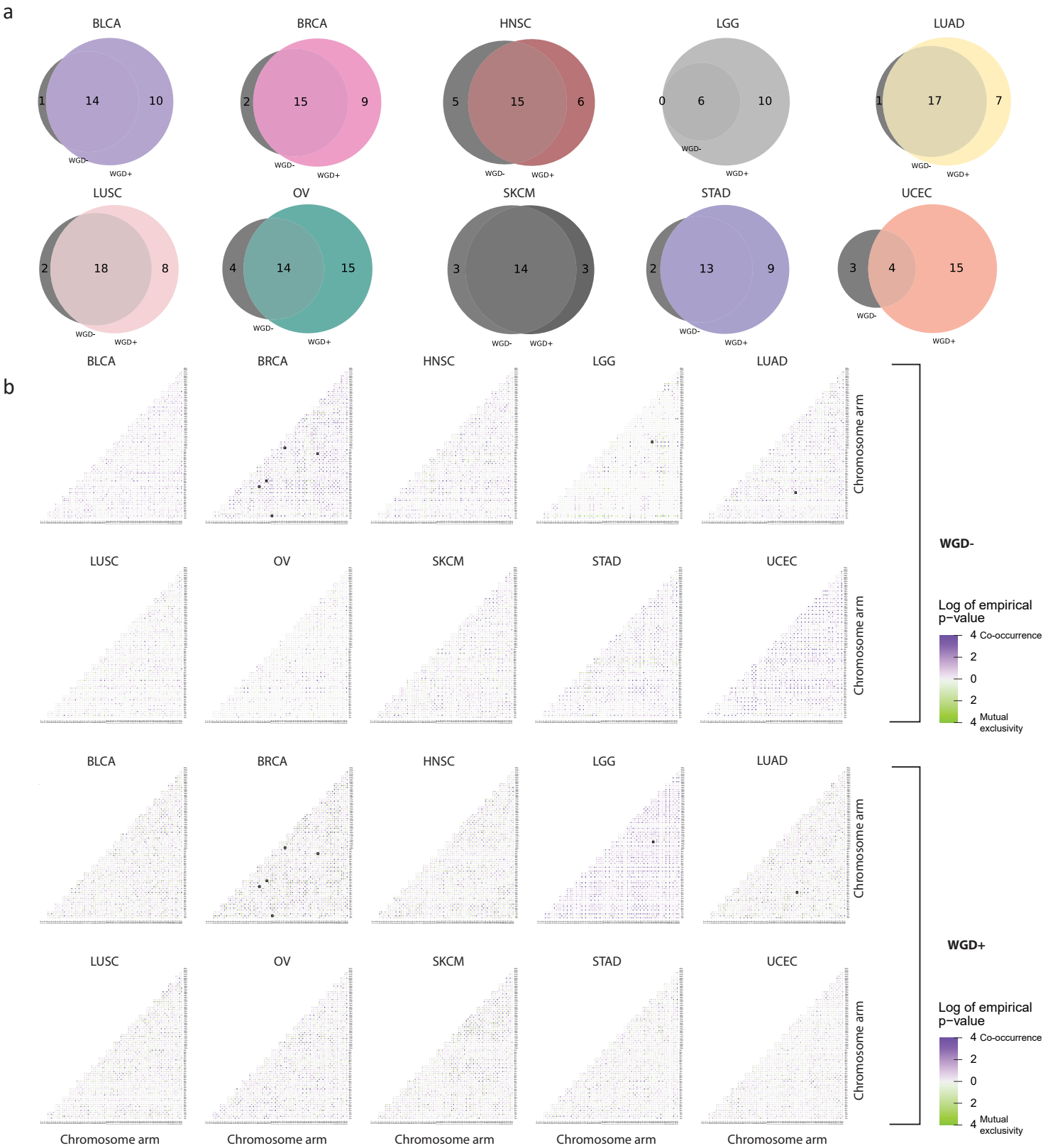

Supplementary Figure 3 page 2

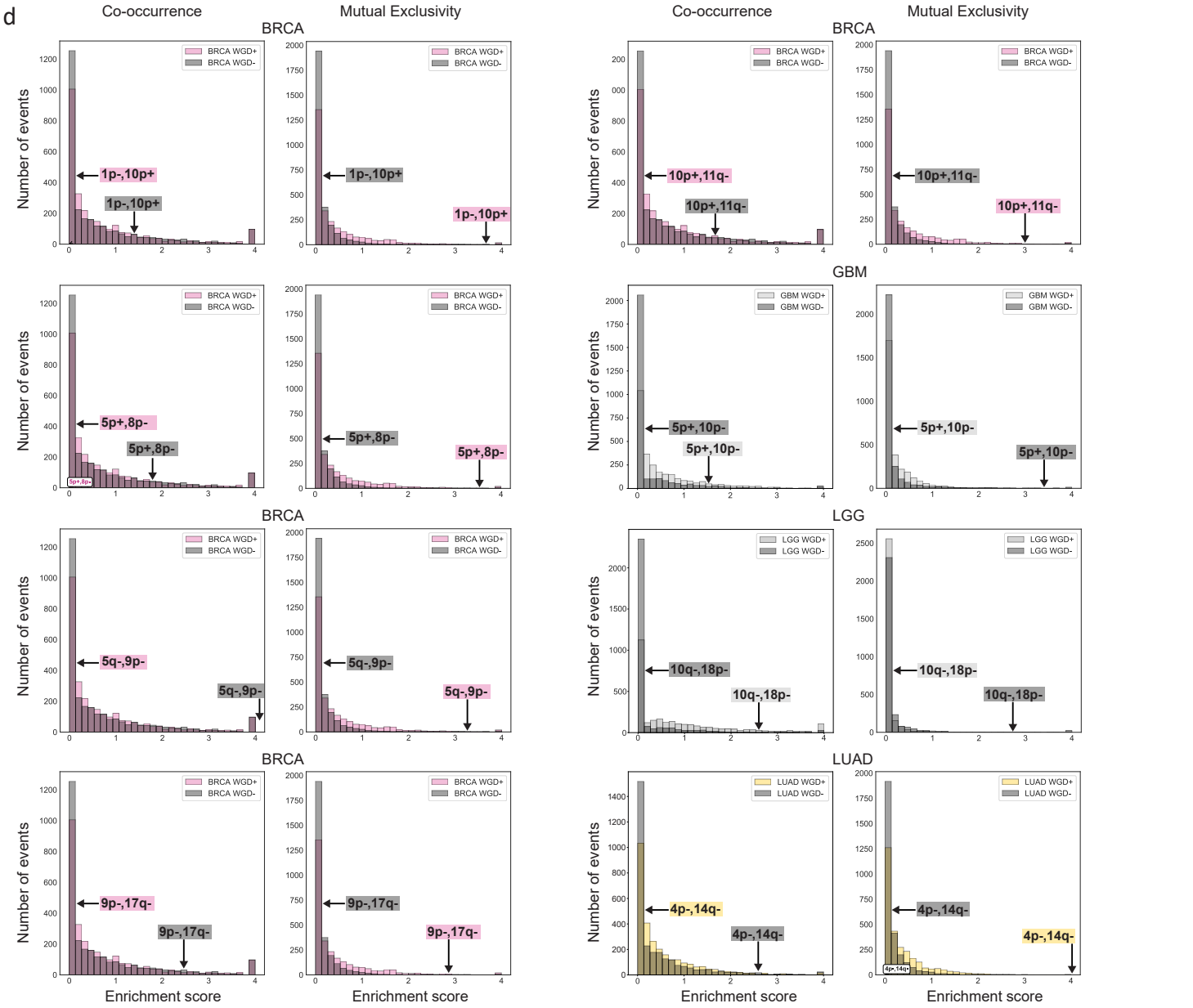

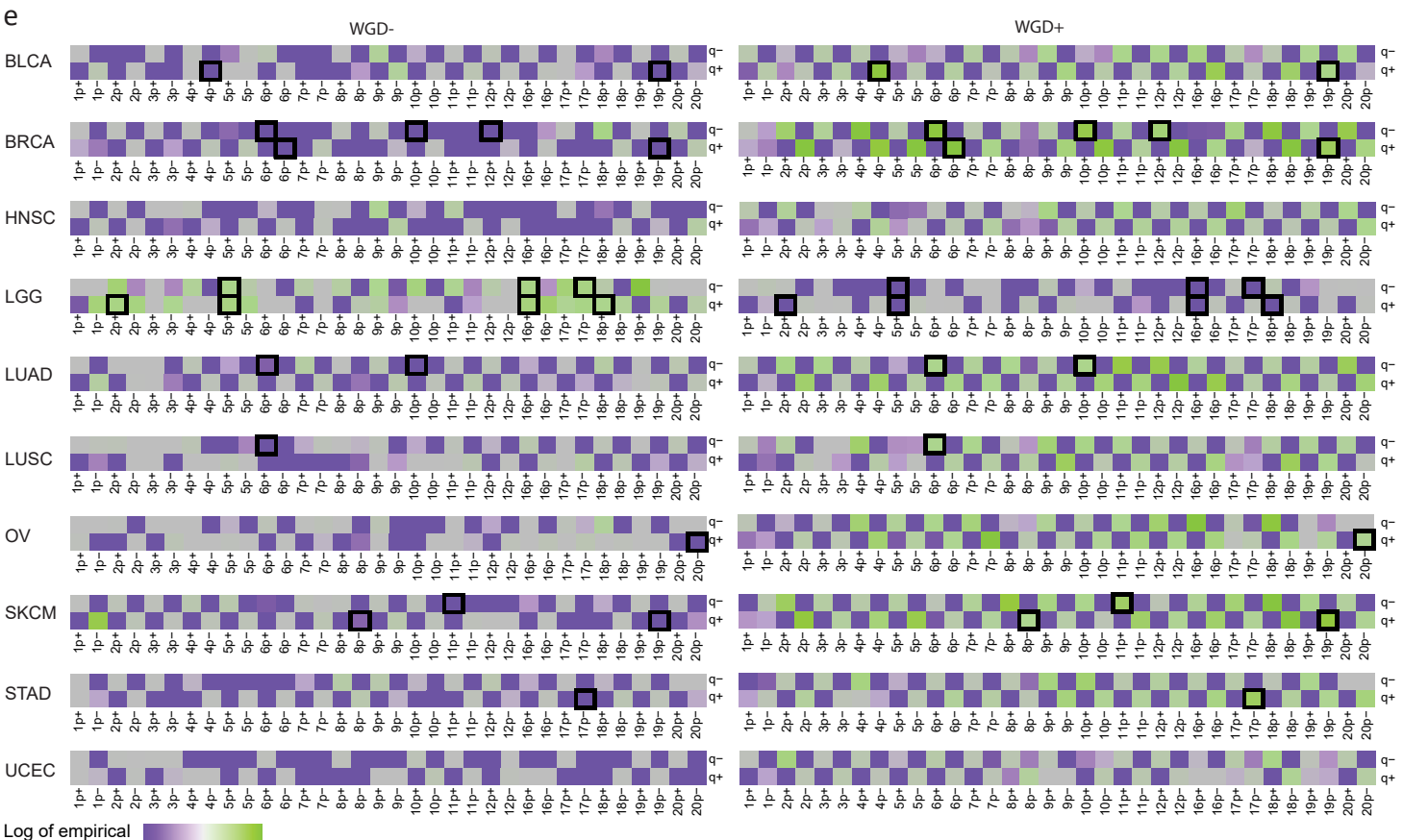

Supplementary Figure 3: WGD is associated with significant changes in pair-wise chromosome-arm genetic interactions (related to Figure 2).

(**a**) Venn diagrams of the number of significant (GISTIC 2.0 q<0.05) chromosome-arm aneuploidies in WGD- and WGD+ tumors of 10 selected tumor types. (**b**) Heatmaps of the significance (-log(empirical p-value)) of positive genetic interactions (co-occurrence, purple) and negative genetic interactions (mutual exclusivity, green) between chromosome arms of different chromosomes in WGD- tumors (top two rows) and WGD+ tumors (bottom two rows) of 10 selected tumor types. Events that were significantly co-occurring in one WGD group but significantly mutually exclusive in the other WGD group of the same tumor type (empirical p<0.05, q<0.25) are highlighted on the heatmaps. (**c**) Venn diagrams of the number of the significantly co-occurring (empirical p<0.05, q<0.25) chromosome-arm inter-chromosomal genetic interactions in WGD- and WGD+ tumors of 10 selected tumor types. (**d**) Histograms of the distribution of enrichment scores (defined as -log(empirical p-value)) for co-occurrence (left) and mutual exclusivity (right) of inter-chromosomal genetic interactions in WGD- vs. WGD+ tumors of BRCA, GBM, LGG and LUAD tumors. Discordant genetic interactions, which are co-occurring in one of the WGD groups but mutually exclusive in the other, are highlighted on the histograms. (**e**) Heatmaps of the significance (-log(empirical p-value)) of positive genetic interactions (co-occurrence, purple) and negative genetic interactions (mutual exclusivity, green) between gains and losses of chromosome arms within the same chromosome in WGD- tumors (left) and WGD+ tumors (right) of 10 selected tumor types. Events that were significantly co-occurring in one WGD group but significantly mutually exclusive in the other WGD group of the same tumor type (empirical p<0.05, q<0.25) are highlighted on the heatmaps. Tumor type abbreviations as in **Fig. 1**.

Supplementary Figure 4

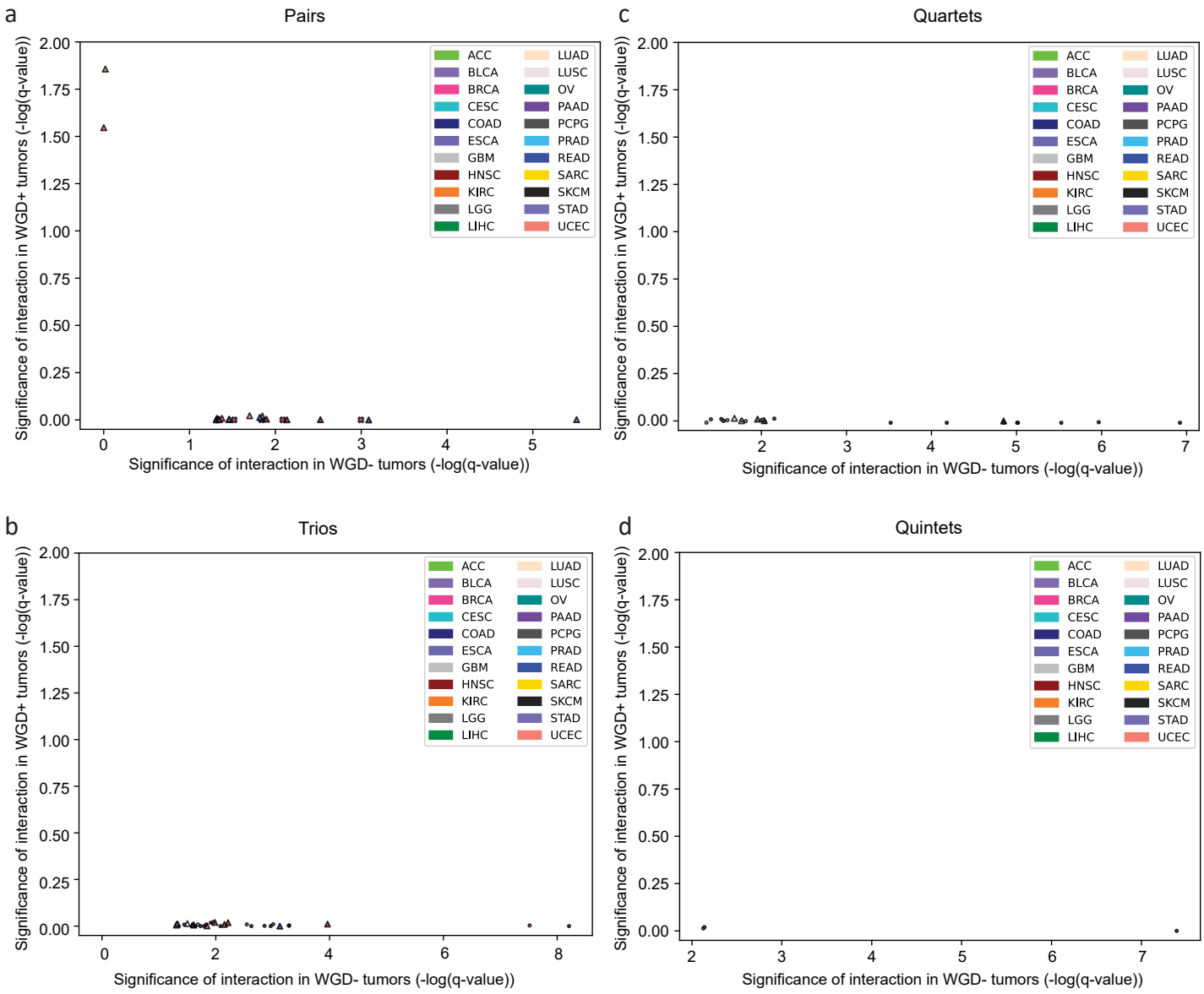

Supplementary Figure 4: WGD is associated with significant changes in multiple chromosome-arm genetic interactions (related to Figure 2).

(**a**) Scatter plots of the significance (-log(q-value)) of positive genetic interactions (co-occurrence) between pairs (n=2) of chromosome arms from different chromosomes in WGD- tumors (x-axis) and WGD+ tumors (y-axis) across tumor types. Interactions that were significantly co-occurring in one WGD group but significantly mutually exclusive in the other WGD group of the same tumor type ($q<0.05$ for one WGD group and $q>0.95$ for the other WGD group) are shown. Interactions are color coded by tumor type (tumor type abbreviations as in **Fig. 1**). Interactions also identified by the permutation analysis are shaped as 'x'. (**b**) Scatter plots of the significance (-log(q-value)) of positive genetic interactions (co-occurrence) between trios (n=3) of chromosome arms from different chromosomes in WGD- tumors (x-axis) and WGD+ tumors (y-axis) across tumor types. Interactions that were significantly co-occurring in one WGD group but significantly mutually exclusive in the other WGD group of the same tumor type ($q<0.05$ for one WGD group and $q>0.95$ for the other WGD group) are shown. Interactions are color coded by tumor type (tumor type abbreviations as in **Fig. 1**). Interactions found to be more significant than any of the subset interactions within them are shaped as triangles. (**c**) as in (**b**), but with quartets (n=4) of chromosome arms. (**d**) as in (**b**) but with quintets (n=5) of chromosome arms.

Supplementary Figure 5

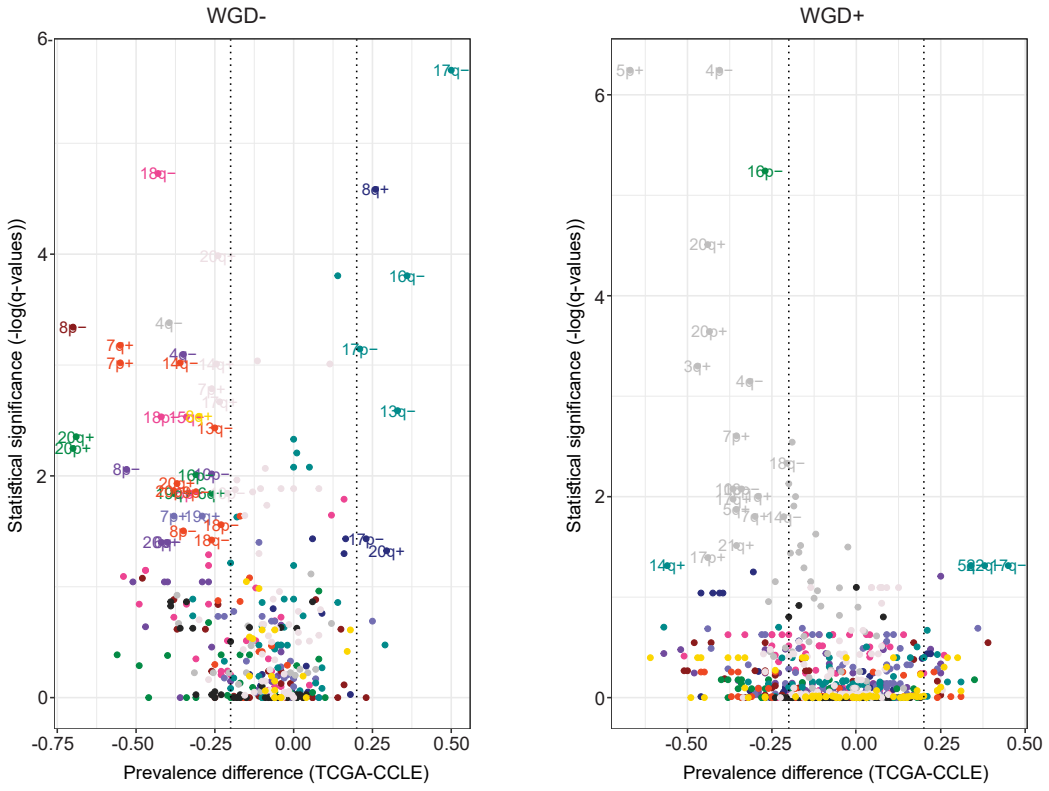

Supplementary Figure 5: Comparison of the aneuploidy landscapes between tumors (TCGA) and cell lines (CCLE) (related to Figure 3).

Volcano plots showing the differential aneuploidy landscapes between tumors and cell lines, for WGD- (left) and WGD+ (right) samples. Events were determined to differentially recur in tumors and in cell lines if the difference in their prevalence was > 0.2 and q-value<0.05 (two-tailed Fisher's Exact test). Only ~11% and ~3% of the recurrent events were discordant between cell lines and tumors, in WGD- and WGD+ samples, respectively. Note that brain cancer cell lines were an exception to this overall high similarity, as several aneuploidies recur in WGD+ CNS cell lines but not in primary brain tumors.

Supplementary Figure 6

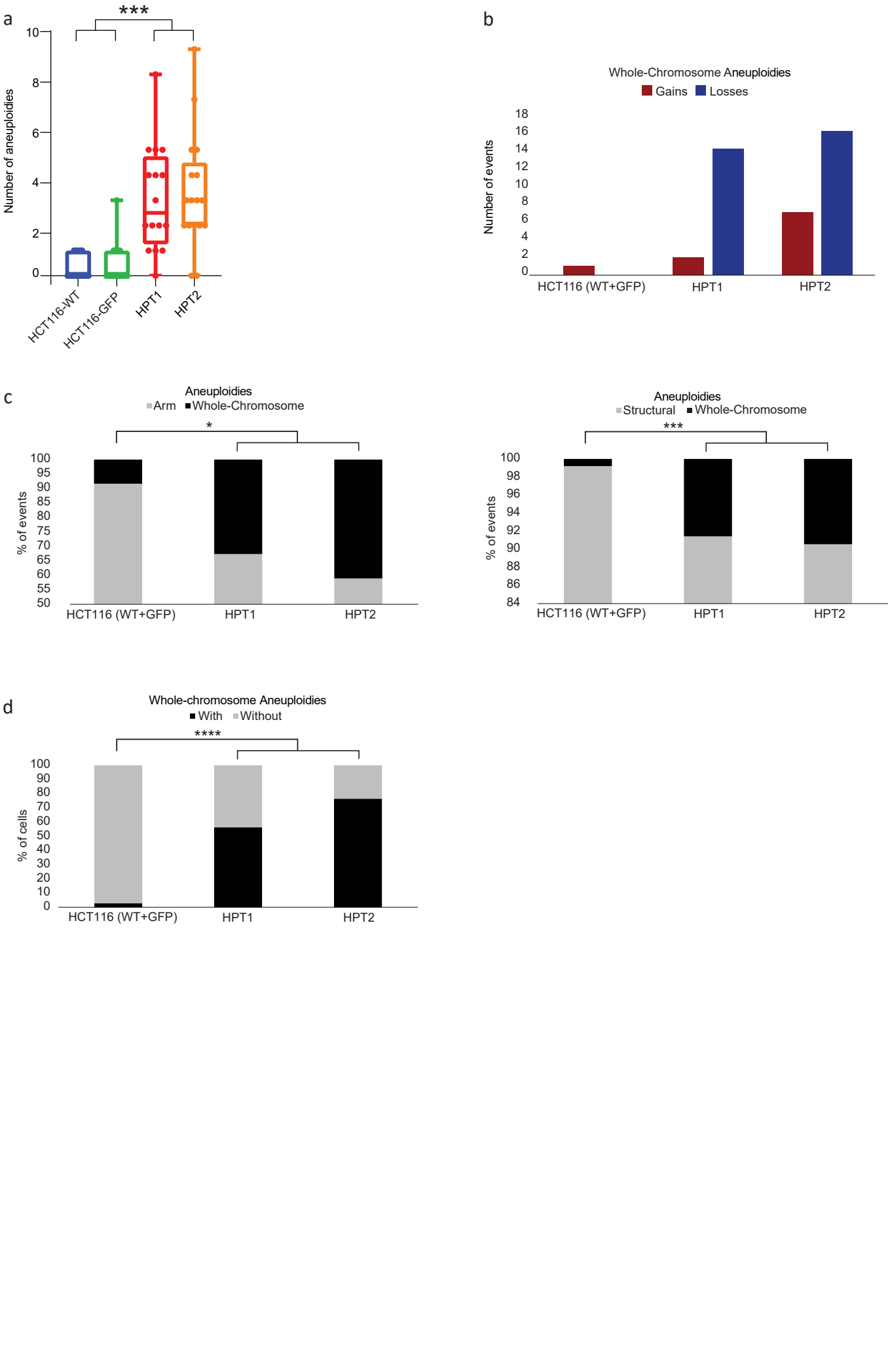

Supplementary Figure 6: Isogenic WGD- and WGD+ HCT116 cell lines demonstrate a causal effect of WGD on aneuploidy landscapes (related to Figure 4).

(**a**) scDNAseq-based comparison of the number of aneuploidies (relative to basal ploidy) between the near-diploid parental HCT116 cells (HCT116-WT), HCT116 cells expressing GFP (HCT116-GFP), and two WGD+ HCT116 clones (HPT1 and HPT2). ***, $p<0.001$; two-tailed Student's t-test. (**b**) The number of whole-chromosome gains and losses observed by mFISH, in HCT116 and its derived WGD+ clones (>20 single cells per clone). (**c**) The relative fraction of whole-chromosome aneuploidies relative to arm-level aneuploidies (left) or structural aneuploidies (right; including arm-level aneuploidies, translocations and smaller structural alterations), in HCT116 and its derived clones. *, $p<0.05$, ***, $p<0.001$; one-tailed Fisher's Exact test. (**d**) The fraction of cells with non-clonal whole-chromosome aneuploidies, a measure of karyotypic heterogeneity, in HCT116 and its derived clones. ****, $p<0.0001$; one-tailed Fisher's Exact test.

Supplementary Figure 7

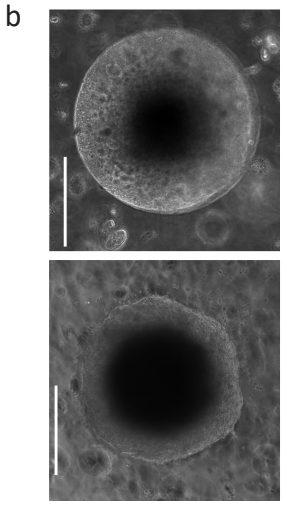

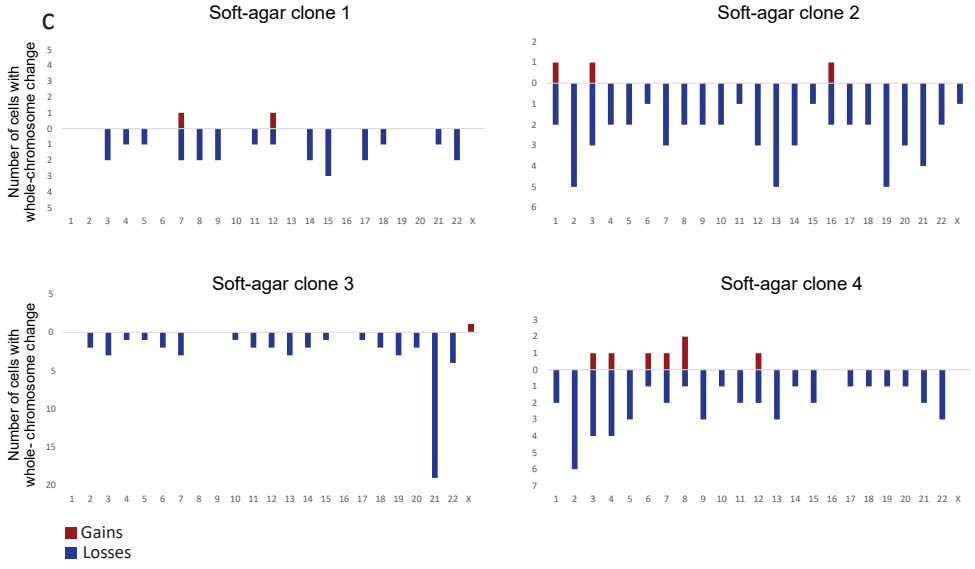

Supplementary Figure 7: Selection pressures result in non-convergent karyotypic evolution (related to Figure 5).

(**a**) Bar plots of the number of cells with gains and losses of each chromosome in the near-diploid parental DLD1 cells (DLD1-parental), and 11 DLD1-derived WGD+ clones. (**b**) Representative images of soft-agar macrocolonies emerging from DLD1 cells evolved for 12 days post-cytokinesis failure. Scale, 500 µM. (**c**) Bar plots of the number of cells with gains and losses of each chromosome in the four profiled soft-agar colonies.

Supplementary Figure 8

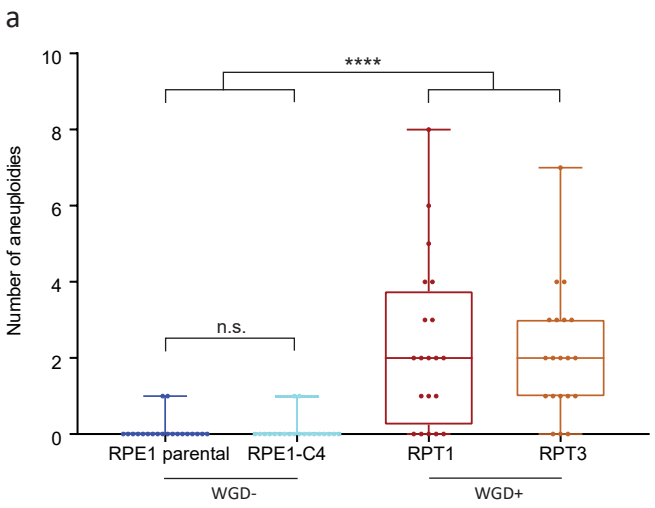

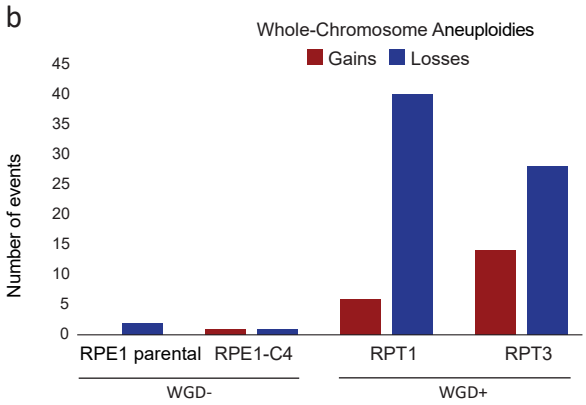

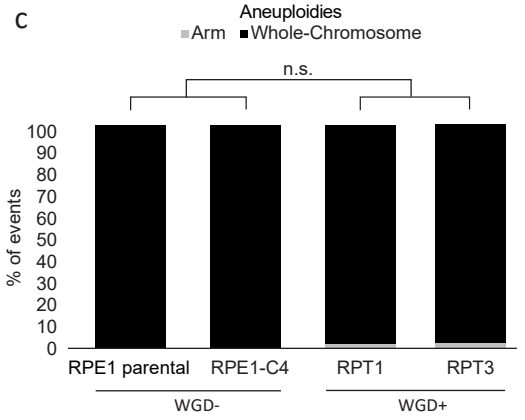

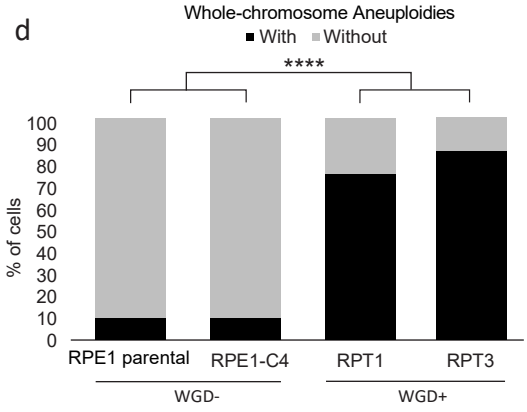

Supplementary Figure 8: Isogenic WGD- and WGD+ RPE1 cell lines demonstrate a causal effect of WGD on aneuploidy landscapes.

(**a**) mFISH-based comparison of the number of aneuploidies (relative to basal ploidy) between near-diploid parental RPE1 cells (RPE1-parental), an RPE1-derived WGD- clone (RPE1-C4), and two RPE1-derived WGD+ clones (RPT1 and RPT3). n.s., $p>0.05$, ****, $p<0.0001$; two-tailed Student's t-test. (**b**) The number of whole-chromosome gains and losses observed by mFISH, in RPE1 and its derived clones (>20 cells per clone). (**c**) The relative fraction of whole-chromosome aneuploidies relative to arm-level aneuploidies in RPE1 and its derived clones. n.s., $p>0.05$; one-tailed Fisher's Exact test. Note that only two aneuploidies were identified in the WGD- RPE1 cells (both in RPE1-parental and in RPE1-C4 cells), rendering this comparison uninformative. (**d**) The fraction of cells with whole-chromosome aneuploidies, a measure of karyotypic heterogeneity, in RPE1 and its derived clones. ****, $p<0.0001$; one-tailed Fisher's Exact test.